

A high frequency builder software for arbitrary radio frequency signals

Cite as: Rev. Sci. Instrum. 93, 034704 (2022); doi: 10.1063/5.0082934

Submitted: 20 December 2021 • Accepted: 21 February 2022 •

Published Online: 21 March 2022



Felix Groß,^{1,a)} Nick Träger,¹ Frank Schulz,¹ Markus Weigand,² Thomas Dippon,³ and Joachim Gräfe^{1,b)}

AFFILIATIONS

¹ Max Planck Institute for Intelligent Systems, 70569 Stuttgart, Germany

² Helmholtz-Zentrum Berlin für Materialien und Energie, 12489 Berlin, Germany

³ Keysight Technologies, 71034 Böblingen, Germany

^{a)} Author to whom correspondence should be addressed: fgross@is.mpg.de

^{b)} Electronic mail: graefe@is.mpg.de

ABSTRACT

While the frequencies accessible by signal generators steadily rise, the synthesization of complex and arbitrary waveforms with high frequency components remains challenging, especially when restricted by an external reference clock. In this article, we present a comprehensive software package combined with state-of-the-art hardware as a solution for the generation of highly sampled, arbitrary radio frequency waveforms. The software can be used to conduct both synchronous and heterodyne pump-probe experiments due to a variety of different synchronization modules. While both kinds of modules allow for standard waveforms, such as sines, pulses, and bursts, as well as any arbitrary signal, the heterodyne modules additionally are not restricted by the reference clock frequency. Both the output and the synchronization module can be adapted to support additional measurement devices. Due to the modular software structure, individual classes can be exchanged while maintaining all functionalities. The software provides a user friendly graphical interface that allows us to compose, save, and load complex arbitrary waveforms within only a few steps. The frequency selectivity provided by the software-hardware combination allows us to directly target specific excitation states of physical systems. Conducting a heterodyne scanning transmission x-ray microscopy experiment, we are able to demonstrate the capabilities of the software when paired with a high sample rate arbitrary waveform generator. The heterodyne synchronization modules allow for unlimited flexibility leveraging arbitrary waveform generation to their full power. By solving the challenges of synthesizing highly complex electromagnetic waves, the software enables a large variety of experiments to be performed more conveniently.

© 2022 Author(s). All article content, except where otherwise noted, is licensed under a Creative Commons Attribution (CC BY) license (<http://creativecommons.org/licenses/by/4.0/>). <https://doi.org/10.1063/5.0082934>

I. INTRODUCTION

Ever since the discovery of electricity and electric currents, the manipulation of electromagnetism has been an essential part of physics, engineering, and technology. At the present time, in the age of information technology, the efficient generation and manipulation of even the tiniest currents has proven to be more important than ever.

Countless physical experiments rely on some sort of electromagnetic radiation. Modern lasers alone¹ are so versatile that basic research as well as numerous technological applications are hard to imagine without them. However, the arbitrary synthesization of complicated electric signals is not trivial and gets

increasingly difficult, the higher the carrier frequency of the signal becomes.

While there are passive and active components capable of synthesizing a large variety of radio frequency (RF) signals, a very convenient solution for the generation of RF signals is arbitrary waveform generators (AWGs). AWGs allow generating completely arbitrary electrical signals much more complex than the most common sine, square, or triangle shapes.

Such AWGs are ideally suited for the generation of electrical signals applied in so-called pump-probe experiments. In a pump-probe experiment, a pump signal raises a physical system into an excited state, while a second probe pulse measures the system's physical properties. The probing pulse provides access to

dynamic observables that directly depend on the pulse characteristics. In a classical pump–probe setup, this is achieved with two lasers. While the first pulse excites the system, a second laser pulse is used to interact with the sample in order to draw conclusions about the system's state. However, neither the first excitation pulse nor the probe pulse necessarily has to be generated by a laser. Another commonly used technique is the generation of an arbitrary electrical pump signal by a signal generator and a probing pulse consisting of x rays.^{2–12} Since the versatility of the method allows for all kinds of time resolved measurement techniques, spectroscopy^{13,14} and microscopy^{15,16} setups are frequently combined with pump–probe experiments. By precisely controlling the delay between the pump and the probe signal, sophisticated techniques allows for nanometer^{4,17–21} and femtosecond^{22–25} resolutions in space and time.

While pump–probe experiments are not as difficult to realize if the pump frequency is an integer multiple of the probing frequency, heterodyne operation²⁶ with almost arbitrary pumping frequencies is technically more difficult to achieve, especially for a fixed probing frequency. In order to achieve flawless working conditions, the signal generator needs to tolerate a certain amount of jitter of the pump signal at its reference in clock. Otherwise, the high frequency signal will not match the pattern expected by the probing pulse, which results in a reduction of signal-to-noise ratio and eventually in loss of measurement signal.

In this work, we present a comprehensive software package capable of generating and synchronizing arbitrary electrical signals for RF experiments. While several default synchronization inputs are already implemented, its modular design ensures extensibility for additional options. Similarly, the output module can be extended to support any device capable of waveform generation that can be accessed via a network interface. The graphical user interface provides easy access for all users and a straightforward way to interact with input and output modules as well as with the waveform selection. This software will be widely applicable to various time resolved measurement setups by providing a modular way of managing synchronization of pump and probe signals.

II. SOFTWARE DESIGN

In order to make complex heterodyne signals more accessible for experiments, the high frequency builder (HiB) program aims to provide capabilities for advanced high frequency waveform generation while maintaining maximum usability. This section will first go into detail on the object oriented architecture and describe the modular structure of HiB, which allows for individually suited extensions. In addition, we will present the basic functionalities of the software as well as the software interface.

A. Architecture and functionalities

A schematic of the software structure can be seen in Fig. 1. Individual classes are framed by rectangles, while utilities and functions are visualized with rounded corners.

As illustrated, HiB is built around the HiB AWG class. This class manages the communication with measurement instruments. The current implementation allows for the direct control of a

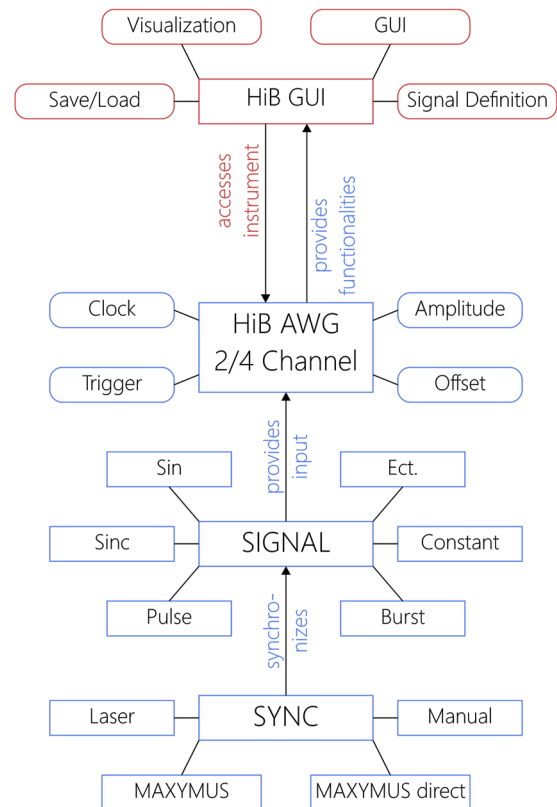


FIG. 1. Illustration of the software architecture: The most central part of the software is the HiB AWG object that is responsible for controlling the signal generator. The HiB GUI object manages user interaction and is responsible for storing and loading save files. The SYNC and SIGNAL classes provide input to the HiB AWG class necessary for signal generation and synchronization.

two- and a four-channel variant of Keysight Technologies M8195A²⁷ AWG. However, due to the modular software design, the class can be easily extended with other output modules supporting different models or even devices from other manufacturers. The HiB AWG module can directly access and manipulate instrument properties, such as the trigger and clock mode and individual offsets of all available channels.

In order to generate a signal, the HiB AWG class receives input from two additional classes, the SIGNAL and the SYNC class. The latter one manages the synchronization of the signal with an external reference clock. Depending on the superclass, the SYNC class allows for either synchronous or heterodyne operation. The current superclasses allow for manual synchronization, synchronization with a pulsed laser, or the synchronization with a time resolved scanning transmission x-ray microscopy setup located at the BESSY II synchrotron radiation facility (MAXYMUS).

The synchronous modes use a multiplier M and only allows for output frequencies that are an integer multiple of the reference clock. For example, if the reference clock is set to 100 MHz, the output can be set to $M \cdot 100$ MHz with $M \in \mathbb{N}$.

In addition to a multiplier M , the heterodyne modes also include a divider N . For a reference clock of 100 MHz, the output frequency can be set to $M/N \cdot 100$ MHz with $(M, N) \in \mathbb{N}$, which gives access to almost all frequencies regardless of the reference clock frequency.

After synchronization is established, the signal is synthesized by the SIGNAL class. The subsequent steps of setting up a signal are plug and play and fully independent from the chosen synchronization. Currently, each signal can consist of the following components: a continuous sine wave, a sinc pulse, a normal pulse, a burst pulse, and a constant offset. Like for the other modules, this selection can be extended at any time. Afterwards, the synthesized signal is passed to the output module that uploads it to the device.

Any user interaction with the program is handled by the HiB GUI (Graphical User Interface) class. It provides utilities such as saving and loading waveforms to a .hib file, visualizes the signal, and manages the user input for signal definition. An additional functionality provided by the HiB GUI, which does not directly correspond to instrument control, is the possibility to display the output signal in the frequency domain. While an ideal signal would only contain the expected frequency components, the interpolation done by the signal generator will not allow for a perfectly synthesized signal. Hence, evaluating the real signal in the frequency domain can be helpful in

order to avoid measurement noise. For example, while an ideal continuous sine wave would only contain one sharp peak at its main frequency, the frequency domain will reveal rapidly decaying intensity next to the main peak. For more complex signals, the frequency verification process is even more important not only to reduce the impact of unwanted signals but also to avoid incorrect user input.

B. Interface example

This section will briefly explain the user interface displayed in Fig. 2 and its basic components. Essentially, the interface consists of a utility section and four main panels, which will be explained in the following.

While HiB will save the synchronization and output module configuration to the users %APPDATA% folder, the utility section on the very top of the interface also allows the user to export the current signals and import previously saved waveforms. While its main focus is exporting and loading files, this section also provides developer information to the user in case anyone runs into problems using the software and considers contacting the authors.

The panel on the left is dedicated to external synchronization. This panel allows for switching between preconfigured synchronization modules or synchronizes to an internal reference clock of the AWG. For heterodyne synchronization, the user input for

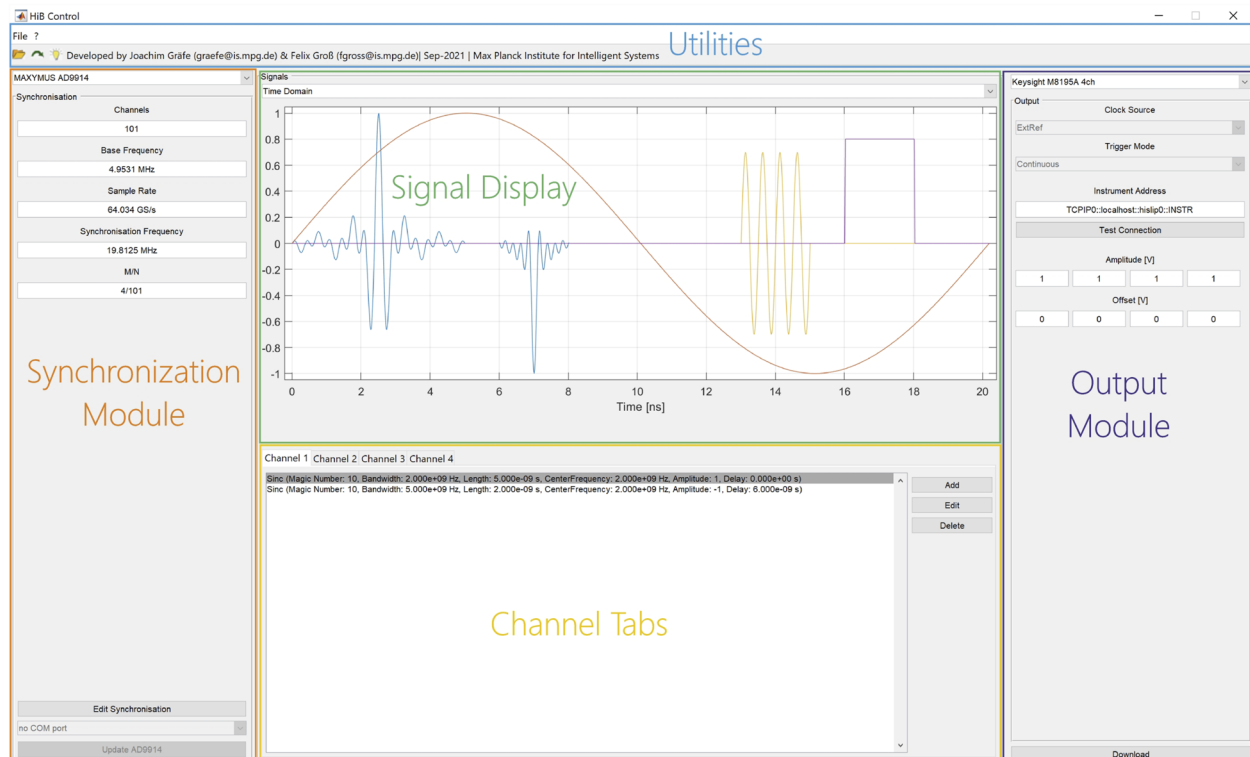


FIG. 2. The software interface consists of four main sections and additional utilities (light blue): The synchronization module (orange) manages the synchronization to an external reference clock, while the output module (purple) directly communicates with the measurement device. The channel (yellow) and signal display (green) allow the user to synthesize and visualize signals.

the divider N is required; otherwise, the software will default to 1, which equals the synchronous mode. The panel also displays useful information such as the base frequency calculated from the divider.

For continuous wave excitation, the multiplier M of each signal is automatically determined when adding a signal to the channel section. For all other signal types, the multiplier can be adapted by the user and determines how long it takes for a signal to be repeated. A standard selection of signals is displayed in the signal panel of Fig. 2 and consists of a sine (orange), a variation of sines (blue), a pulse (purple), a burst (yellow), and a constant voltage offset. The amount of output channels changes depending on the AWG configuration while each channel can be controlled individually. The drop-down list in the signal display switches between time and frequency domain representation of the signals.

The output panel on the right side of the interface manages the AWG device communication. The drop-down list at the top allows us to choose the output module. Currently implemented modules include Keysight Technologies' two- and four-channel version M8195A;²⁷ however, the output module can easily be extended to any AWG, provided it has a network interface. In addition, the panel displays the current clock source and trigger mode. A connection to the output device can be opened via the *Test Connection* button, which also indicates whether a connection could be established. With the amplitude and offset boxes, the overall amplitude of each channel can be changed. Finally, after carefully checking all synchronization, signal, and device parameters, the download button at the bottom of the panel establishes a connection to the device and uploads the waveform. If an error occurs during the upload process, a popup message guides the user and helps the user to identify possible sources of the problem. If the upload is finished successfully, signal generation is started immediately.

III. EXPERIMENTAL PUMP-PROBE EXAMPLE

As an experimental example, we include a spin wave movie recorded at the scanning transmission x-ray microscope (STXM) MAXYMUS, which is part of the BESSY II synchrotron radiation facility in Berlin. The locking of the AWG reference clock to the synchrotron frequency is not trivial and includes an additional prescaler P and fractional divider F . However, all these are managed by the HiB software and not something the user has to take care of. For more information, the reader is referred to Ref. 11.

A schematic of the experimental setup is displayed in Fig. 3(a). The AWG is connected to the sample either directly or via an additional RF amplifier. The setup allows us to drive and measure the sample with arbitrarily complex pump signals. The output of the sample is connected to a fast oscilloscope to monitor the control signal. While driving the sample with a pump signal, it gets simultaneously probed with x-ray flashes, which are synchronized to the AWG output. This allows for the direct imaging of magnetization dynamics via the x-ray magnetic circular dichroism effect.²⁸ For a more thorough introduction on how to measure magnetization dynamics, the reader is referred to Refs. 6 and 11.

The HiB software allows us to tailor the pump signal to be any arbitrary composition of frequencies. HiB directly connects to the synchrotron setup, and the heterodyne synchronization allows us to sample any arbitrary signal as input for the experiment. Hence, the

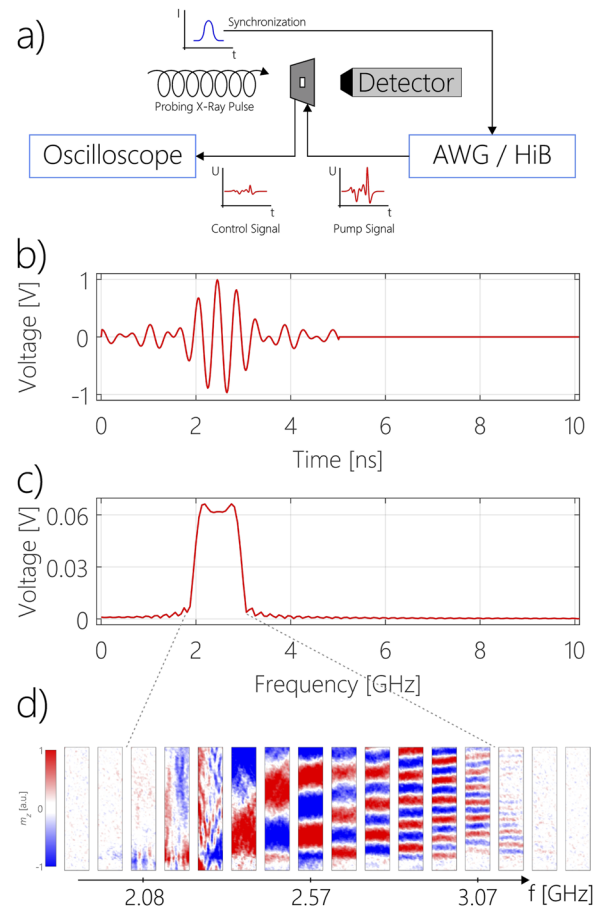


FIG. 3. Experimental verification with a complex waveform: (a) Schematic of the experimental setup. (b) Input signal generated by the combination of AWG and HiB. (c) Input signal displayed in frequency space. (d) Magnonic response of the system to a high frequency excitation ranging from 2 to 3 GHz.

here presented solution is much more versatile and flexible when it comes to the generation and synchronization of complex RF signals than conventional pump methods.

As an example, a precisely tailored sinc function [Fig. 3(b)] is able to evenly distribute input power over an arbitrarily large frequency range [Fig. 3(c)].⁸ The tailored sinc function has a bandwidth of 1 GHz and a center frequency of 2.5 GHz and is used to equally excite spin waves between 2 and 3 GHz. This signal can be directly synthesized with only a few clicks using the HiB software and an arbitrary waveform generator. Otherwise, such a waveform would require multiple active and passive components all combined to a single RF setup. In addition, the software not only manages the instrument communication with the AWG but also ensures that the output and reference signal are correctly synchronized.

Figure 3(d) displays snapshots of the measured m_z -component of the dynamic magnetization. The experimental results confirm that the setup is working as intended. For frequencies outside of the 2–3 GHz range, the spin wave system displays hardly any response due to the low input power at these frequencies. Judging

from the wave length being continuously reduced when increasing the frequency, we can confirm that the signal corresponds to an actual system response and is not caused by measurement artifacts. Hence, the presented method can be used not only to directly excite desired frequencies but also to exclude possibly unwanted frequencies known to contribute exclusively to a more noisy measurement signal.

Beyond the data presented here, the software was successfully utilized for spin wave^{5,8,12,21,29–33} and space time crystal imaging.²⁰ Its versatility and accessibility facilitate the generation of complex high-frequency signals, which is of great benefit to scientists in all disciplines.

IV. CONCLUSIONS

In this article, we presented a software–hardware combination capable of generating complex waveforms with high precision. HiB provides a modular software architecture while maintaining a user friendly interface design. The predefined synchronization and output modules can either be used as intended, adapted, or completely redesigned according to the user's needs, enabling communication with a wide range of measuring devices.

Depending on the type of experiment, the synchronization module allows for either synchronous or heterodyne operation, enabling the software to run with a large variety of different experiments. By combining a frequency multiplier and divider, the software allows not only the sampling of any continuous wave, pulse, burst, or sinc signal but also enables the realization of pump–probe experiments with any arbitrary signal, independent from the synchronization module. Each of the output channels can generate independent waveforms with customizable amplitudes, offsets, and delays, while the interface provides a clean overview over the current instrument output and allows for the export and import of waveform save files. Hence, the software offers maximum flexibility while maintaining an easily accessible user interface.

To demonstrate the capabilities of HiB, we presented a heterodyne pump–probe experiment that is highly susceptible to the stability of the pump signal with respect to the reference clock. The complex waveform generated by the AWG allows us to excite nanosecond magnetization dynamics with arbitrarily selected frequencies. We expect the software to be used in a large variety of pump–probe experiments due to its extensibility and versatility while also lowering the entry barrier for the generation of complex radio frequency waveforms to unprecedented levels.

SUPPLEMENTARY MATERIAL

See the [supplementary material](https://gitlab.gwdg.de/moketeam/hib/-/tree/master) for the HiB software (<https://gitlab.gwdg.de/moketeam/hib/-/tree/master>) and a tutorial (<https://gitlab.gwdg.de/moketeam/hib/-/tree/master/Tutorial>) both of which can be downloaded from GitLab.

ACKNOWLEDGMENTS

The authors thank Ulrike Eigenthaler and Thomas Meisner for sample preparation and Sebastian Wintz for support during beam

times. They also thank HZB for allocation of synchrotron radiation beamtime at the MAXYMUS end station.

AUTHOR DECLARATIONS

Conflict of Interest

The authors declare no conflict of interest.

DATA AVAILABILITY

Raw data were generated at the BESSY II synchrotron radiation facility. Derived data supporting the findings of this study are available from the corresponding author upon reasonable request.

REFERENCES

- 1 P. A. Franken, A. E. Hill, C. W. Peters, and G. Weinreich, *Phys. Rev. Lett.* **7**(4), 118–119 (1961).
- 2 J. J. van Thor and A. Madsen, *Struct. Dyn.* **2**(1), 014102 (2015).
- 3 F. Groß, M. Zelent, A. Gangwar, S. Mamica, P. Gruszecki, M. Werner, G. Schütz, M. Weigand, E. J. Goering, C. H. Back, M. Krawczyk, and J. Gräfe, *Appl. Phys. Lett.* **118**(23), 232403 (2021).
- 4 S. Wintz, V. Tiberkevich, M. Weigand, J. Raabe, J. Lindner, A. Erbe, A. Slavin, and J. Fassbender, *Nat. Nanotechnol.* **11**(11), 948–953 (2016).
- 5 N. Träger, P. Gruszecki, F. Lisiecki, F. Groß, J. Förster, M. Weigand, H. Głowiński, P. Kuświk, J. Dubowik, M. Krawczyk, and J. Gräfe, *Nanoscale* **12**(33), 17238–17244 (2020).
- 6 F. Groß, N. Träger, J. Förster, M. Weigand, G. Schütz, and J. Gräfe, *Appl. Phys. Lett.* **114**(1), 012406 (2019).
- 7 F. J. Willeumier and M. Meyer, *J. Phys. B: At., Mol. Opt. Phys.* **39**(23), R425–R477 (2006).
- 8 N. Träger, F. Groß, J. Förster, K. Baumgaertl, H. Stoll, M. Weigand, G. Schütz, D. Grundler, and J. Gräfe, *Sci. Rep.* **10**(1), 18146 (2020).
- 9 K. Litzius, I. Lemesch, B. Krüger, P. Bassirian, L. Caretta, K. Richter, F. Büttner, K. Sato, O. A. Tretiakov, J. Förster, R. M. Reeve, M. Weigand, I. Bykova, H. Stoll, G. Schütz, G. S. D. Beach, and M. Kläui, *Nat. Phys.* **13**(2), 170–175 (2016).
- 10 J. Förster, J. Gräfe, J. Bailey, S. Finizio, N. Träger, F. Groß, S. Mayr, H. Stoll, C. Dubs, O. Surzhenko, N. Liebing, G. Woltersdorf, J. Raabe, M. Weigand, G. Schütz, and S. Wintz, *Phys. Rev. B* **100**(21), 214416 (2019).
- 11 J. Gräfe, M. Weigand, B. Van Waeyenberge, A. Gangwar, F. Groß, F. Lisiecki, J. Rychly, H. Stoll, N. Träger, J. Förster, F. Stobiecki, J. Dubowik, J. Klos, M. Krawczyk, C. H. Back, E. J. Goering, and G. Schütz, *Proc. SPIE* **11090**, 1109025 (2019).
- 12 F. Groß, N. Träger, and J. Gräfe, *SoftwareX* **15**, 100705 (2021).
- 13 G. Khitrova, P. R. Berman, and M. Sargent, *J. Opt. Soc. Am. B* **5**(1), 160–170 (1988).
- 14 S. Woutersen, U. Emmerichs, and H. J. Bakker, *Science* **278**(5338), 658–660 (1997).
- 15 M. C. Fischer, J. W. Wilson, F. E. Robles, and W. S. Warren, *Rev. Sci. Instrum.* **87**(3), 031101 (2016).
- 16 P.-T. Dong and J.-X. Cheng, *Spectroscopy* **32**(4), 2–11 (2017); available at <https://www.spectroscopyonline.com/view/pump-probe-microscopy-theory-instrumentation-and-applications>.
- 17 E. M. Grumstrup, M. M. Gabriel, E. E. M. Cating, E. M. Van Goethem, and J. M. Papanikolas, *Chem. Phys.* **458**, 30–40 (2015).
- 18 F. Lisiecki, J. Rychly, P. Kuświk, H. Głowiński, J. W. Klos, F. Groß, I. Bykova, M. Weigand, M. Zelent, E. J. Goering, G. Schütz, G. Gubbiotti, M. Krawczyk, F. Stobiecki, J. Dubowik, and J. Gräfe, *Phys. Rev. Appl.* **11**(5), 054003 (2019).
- 19 F. Lisiecki, J. Rychly, P. Kuświk, H. Głowiński, J. W. Klos, F. Groß, N. Träger, I. Bykova, M. Weigand, M. Zelent, E. J. Goering, G. Schütz, M. Krawczyk, F. Stobiecki, J. Dubowik, and J. Gräfe, *Phys. Rev. Appl.* **11**(5), 054061 (2019).
- 20 N. Träger, P. Gruszecki, F. Lisiecki, F. Groß, J. Förster, M. Weigand, H. Głowiński, P. Kuświk, J. Dubowik, G. Schütz, M. Krawczyk, and J. Gräfe, *Phys. Rev. Lett.* **126**(5), 057201 (2021).

- ²¹F. Groß, M. Zelent, N. Träger, J. Förster, U. T. Sanli, R. Sauter, M. Decker, C. H. Back, M. Weigand, K. Keskinbora, G. Schütz, M. Krawczyk, and J. Gräfe, *ACS Nano* **14**(12), 17184–17193 (2020).
- ²²C. Stamm, T. Kachel, N. Pontius, R. Mitzner, T. Quast, K. Holldack, S. Khan, C. Lupulescu, E. F. Aziz, M. Wietstruk, H. A. Dürr, and W. Eberhardt, *Nat. Mater.* **6**(10), 740–743 (2007).
- ²³C. Stamm, N. Pontius, T. Kachel, M. Wietstruk, and H. A. Dürr, *Phys. Rev. B* **81**(10), 104425 (2010).
- ²⁴J. M. Glowina, J. Cryan, J. Andreasson, A. Belkacem, N. Berrah, C. I. Blaga, C. Bostedt, J. Bozek, L. F. DiMauro, L. Fang, J. Frisch, O. Gessner, M. Gühr, J. Hajdu, M. P. Hertlein, M. Hoener, G. Huang, O. Kornilov, J. P. Marangos, A. M. March, B. K. McFarland, H. Merdji, V. S. Petrovic, C. Raman, D. Ray, D. A. Reis, M. Trigo, J. L. White, W. White, R. Wilcox, L. Young, R. N. Coffee, and P. H. Bucksbaum, *Opt. Express* **18**(17), 17620–17630 (2010).
- ²⁵K. Holldack, J. Bahrtdt, A. Balzer, U. Bovensiepen, M. Brzhezinskaya, A. Erko, A. Eschenlohr, R. Follath, A. Firsov, W. Frentrop, L. Le Guyader, T. Kachel, P. Kuske, R. Mitzner, R. Müller, N. Pontius, T. Quast, I. Radu, J.-S. Schmidt, C. Schüßler-Langeheine, M. Sperling, C. Stamm, C. Trabant, and A. Föhlich, *J. Synchrotron Radiat.* **21**(5), 1090–1104 (2014).
- ²⁶M. Heuck, S. Combrié, G. Lehoucq, S. Malaguti, G. Bellanca, S. Trillo, P. T. Kristensen, J. Mørk, J. P. Reithmaier, and A. De Rossi, *Appl. Phys. Lett.* **103**(18), 181120 (2013).
- ²⁷Keysight technology M8195A product page, <https://www.keysight.com/us/en/product/M8195A/65-gsa-s-arbitrary-waveform-generator.html>; accessed 06 09 2021.
- ²⁸G. Schütz, W. Wagner, W. Wilhelm, P. Kienle, R. Zeller, R. Frahm, and G. Materlik, *Phys. Rev. Lett.* **58**(7), 737–740 (1987).
- ²⁹G. Talmelli, T. Devolder, N. Träger, J. Förster, S. Wintz, M. Weigand, H. Stoll, M. Heyns, G. Schütz, I. P. Radu, J. Gräfe, F. Ciubotaru, and C. Adelmann, *Sci. Adv.* **6**(51), eabb4042 (2020).
- ³⁰K. Baumgaertl, J. Gräfe, P. Che, A. Mucchietto, J. Förster, N. Träger, M. Bechtel, M. Weigand, G. Schütz, and D. Grundler, *Nano Lett.* **20**(10), 7281–7286 (2020).
- ³¹N. Träger, P. Gruszecki, F. Lisiecki, J. Förster, M. Weigand, S. Wintz, H. Stoll, H. Głowiński, P. Kuświk, M. Krawczyk, and J. Gräfe, *Phys. Status Solidi RRL* **14**(12), 2000373 (2020).
- ³²S. Mayr, L. Flajšman, S. Finizio, A. Hrabec, M. Weigand, J. Förster, H. Stoll, L. J. Heyderman, M. Urbánek, S. Wintz, and J. Raabe, *Nano Lett.* **21**(4), 1584–1590 (2021).
- ³³N. Träger, F. Lisiecki, R. Lawitzki, M. Weigand, H. Głowiński, G. Schütz, G. Schmitz, P. Kuświk, M. Krawczyk, J. Gräfe, and P. Gruszecki, *Phys. Rev. B* **103**(1), 014430 (2021).